International Journal of Thermal Sciences 48 (2009) 1800–1813

Contents lists available at ScienceDirect

International Journal of Thermal Sciences

journal homepage: www.elsevier.com/locate/ijts

Influence of chemical reaction and thermal radiation on the heat and mass transfer in MHD micropolar flow over a vertical moving porous plate in a porous medium with heat generation

R.A. Mohamed*, S.M. Abo-Dahab [1]

Maths. Dept., Faculty of Science, Qena 83523, Egypt

ARTICLE INFO

Article history:
Received 25 April 2008
Received in revised form
21 January 2009
Accepted 21 January 2009
Available online 21 March 2009

Keywords:
MHD
Micropolar
Thermal radiation
Heat generation
Chemical reaction

ABSTRACT

An analysis is presented for the effects of chemical reaction and thermal radiation on hydromagnetic free convection heat and mass transfer for a micropolar fluid via a porous medium bounded by a semi-infinite vertical porous plate in the presence of heat generation. The plate moves with a constant velocity in the longitudinal direction and the free stream velocity follows an exponentially small perturbation law. A uniform magnetic field acts perpendicularly to the porous surface in which absorbs the micropolar fluid with a suction velocity varying with time. Analytical expressions are computed numerically. Numerical calculations are carried out the purpose of the discussion of the results which are shown on graphs and the effects of the various dimensionless parameters entering into the problem on the velocity, angular velocity, temperature, concentration. Also, the results of the skin-friction coefficient, the couple stress coefficient and the rates of the heat and mass transfers at the wall are prepared with various values of fluid properties and the flow conditions are studied.

1. Introduction

The theory of micropolar has received great attentions during the recent years, because of traditional Newtonian fluids can't precisely describe the characteristic of fluid with suspended particles. Physically, micropolar fluids may present the non-Newt onian fluids consisting of dumb-bell molecules or short rigid cylindrical elements, polymer fluids, fluids suspensions and animal blood. The presence of dust or smoke particular in a gas may also be modeled using micropolar fluid dynamics. Eringen [1] first derived the theory of micropolar fluids, which describe the microrotation effects to the microstructures. Since, Navier–Stockes theory does not describe previously the physical properties of polar fluids, colloidal solutions, suspension solutions, liquid crystals and fluid containing small additives. Eringen [2] extended his theory to the theory of thermomicropolar fluids, which interest to the effects of microstructures on the fluid flow. The mathematical theory of equations of micropolar fluids and applications of these fluids in the theory of lubrication and in the theory of porous media are dealt in recent book by Lukaszewicz [3].

The problem of micropolar fluids through a porous media has many applications such as, porous rocks, foams and foamed solids, aerogels, alloys, polymer blends and microemulsions. Raptis [4] studied boundary layer flow of a micropolar fluid through a porous medium by using the generalized Darcy law. Helmy [5] investigated unsteady free convection flow of a polar fluid through a porous medium where they showed that coupled stress velocity increases resulted in a decrease in the flow velocity. Kim [6] studied unsteady free convection flow of micropolar fluids through a porous medium bounded by an infinite vertical plate. Aganovic and Tutek [7] studied the homogenization of micropolar fluid through a porous medium in mathematical modeling of flow through porous media. Sharma and Gupta [8] studied the effects of medium permeability on thermal convection in micropolar fluids. Hassanien et al. [9] studied natural convection flow over a semi-infinite plate maintained at a constant heat flux embedded in a saturated porous medium of micropolar fluid. Ibrahim et al. [10] studied non-classical thermal effects in Stokes second problem for micropolar fluids by using perturbation method. Ibrahim et al. [11] investigated unsteady magneto-hydrodynamic micropolar fluid flow and heat transfer over a vertical porous plate through a porous medium in the presence of thermal and mass diffusion with constant heat source. Kim [12] investigated MHD convection flow of polar fluids past a vertical moving porous plate in a porous medium.

* Corresponding author. Tel: +20 965210619; fax: +20 965211279.
E-mail addresses: rabdalla_1953@yahoo.com (R.A. Mohamed), sdahb@yahoo.com (S.M. Abo-Dahab).
[1] Tel.: +20 128893470.

1290-0729/$ – see front matter © 2009 Elsevier Masson SAS. All rights reserved.
doi:10.1016/j.ijthermalsci.2009.01.019

Nomenclature

B_0	magnetic induction, tesla
C^*	species concentration, mol m^{-3}
C^*_ω	surface concentration, mol m^{-3}
C^*_∞	species concentration far from the surface, mol m^{-3}
C_f	skin-friction coefficient
C_m	couple stress coefficient
c_p	specific heat at constant pressure, J kg^{-1} K^{-1}
D^*	chemical molecular diffusivity, m^2 s^{-1}
Gm	solutal Grashof number
Gr	Grashof number
g	acceleration due to the gravity, m s^{-2}
H	dimensionless heat generation/absorption coefficient
j^*	microinertia per unit mass, m^2
K^*	permeability of the porous media, m^2
K^*_1	mean absorption coefficient, m^{-1}
K	dimensionless permeability
k	thermal conductivity of the fluid, W m^{-1} K^{-1}
M	local magnetic field parameter
n	parameter related to microgyration vector and shear stress
N	model parameter
Nu	Nusselt number
P^*	pressure, kg m^{-1} s^{-2}
Pr	fluid Prandtl number
Q_0	heat generation coefficient, W m^{-3} K^{-1}
q^*_r	radiative heat flux, W m^{-2}
R^*	reaction rate constant, J
R	radiation parameter
Re	Reynolds number
Sc	generalized Schmidt number
Sh	Sherwood number
t^*	time, s
t	dimensionless time
T^*	temperature in the boundary layer, K
T^*_∞	temperature far away from the plate, K
T^*_w	temperature at the wall, K
u	dimensionless velocity
u^*, v^*	are the velocities along and perpendicular to the plate, m s^{-1}
U_0	scale of free stream velocity
U^*_∞	free stream velocity, m s^{-1}
u^*_p	wall dimensional velocity, m s^{-1}
U_p	wall dimensionless velocity
V_0	scale of suction velocity
x^* and y^*	are the distances along and perpendicular to the plate respectively, m
y	dimensionless spanwise coordinate normal to the plate
α	fluid thermal diffusivity, m^2 s^{-1}
β	ratio of vortex viscosity and dynamic viscosity
β_c	volumetric coefficient of thermal expansion, K^{-1}
β_f	volumetric coefficient of expansion with concentration, K^{-1}
γ	spin – gradient velocity, kg m s^{-1}
δ	scalar constant
ϵ	scalar constant
θ	dimensionless temperature
ζ	chemical reaction parameter
η	scalar constant
μ	fluid dynamic viscosity, kg m^{-1} s^{-1}
ν	fluid kinematic rotational viscosity, m^2 s^{-1}
ν_r	kinematic rotational viscosity, m^2 s^{-1}
ρ	fluid density, kg m^{-3}
σ	electrical conductivity of the fluid, S m^{-1}
σ^*	Stefan–Boltzmann constant, W m^{-2} K^{-4}
ω	angular velocity vector, m s^{-1}
Γ	coefficient of gryo-viscosity (or vortex viscosity), kg m^{-1} s^{-1}

Many processes in new engineering areas occur at high temperatures and knowledge of radiate heat transfer becomes very important for the design of the pertinent equipment. Nuclear power plants gas turbines and the various propulsion devices for aircraft, missiles, satellites and space vehicles are examples of such engineering areas. The study of radiation effects on the various types of flows is quite complicated. In the recent years, many authors have studied radiation effects on the boundary layer of radiating fluids past a plate. Raptis [13] studied the flow of a micropolar fluid past continuously moving plate by the presence of radiation. The radiation effect on heat transfer of a micropolar fluid past unmoving horizontal plate through a porous medium was studied by Abo-Eldahab and Ghonaim [14]. Kim and Fedorov [15] investigated the transient mixed radiative convection flow of a micropolar fluid past a moving semi-infinite vertical porous plate.

The micropolar fluid considered here is a gray, absorbing–emitting but non-scattering medium. The Rosseland approximation is used to describe the radiative heat flux in the energy equation. It is also assumed that the porous plate moves with constant velocity in the longitudinal direction, and the free stream velocity flows on exponentially small perturbation law.

Convection problems associated with heat sources within fluid-saturated porous media are of great practical significance, for there are a number of practical applications in geophysics and energy-related problems, such as recovery of petroleum resources, geophysical flows, cooling of underground electric cables, storage of nuclear waste materials ground water pollution, fiber and granular insulations, solidification of costing, chemical catalytic reactors and environmental impact of buried heat generating waste. Abo-Eldahab and El-Aziz [16] investigated the problem of steady, laminar, free convection boundary layer flow of a micropolar fluid from a vertical stretching surface embedded in a non-Darcing porous medium in the presence of a uniform magnetic

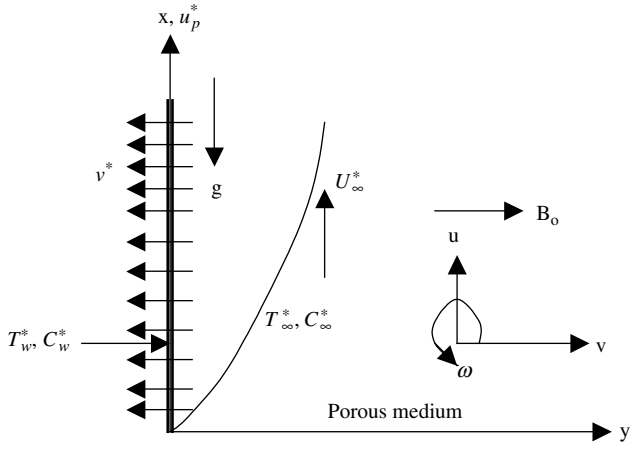

Fig. 1. Physical model and coordinate system of the problem.

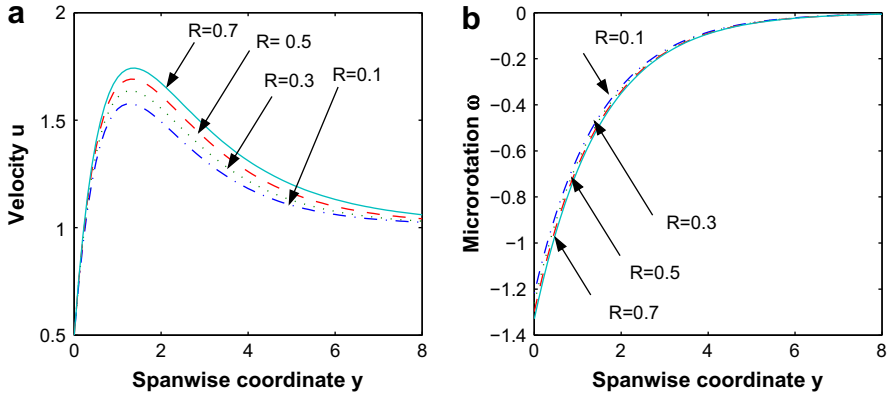

Fig. 2. Velocity and Microrotation profiles for various values of R with $n = 0.5$, $Sc = 0.2$, $M = 2$, $Gr = 2$, $Gc = 2$, $K = 2$, $Pr = 1$, $Up = 0.5$, $H = 0.1$, $\zeta = 1$ and $\beta = 0.5$.

field, heat generation/absorption and free stream velocity. Gorla et al. [17] have presented an analysis for the unsteady natural convection from a heated vertical surface placed in a micropolar fluid in the presence of internal heat generation or absorption.

Combined heat and mass transfer problems with chemical reaction are of importance in many processes and have, therefore, received a considerable amount of attention in recent years. In processes such as drying, evaporation at the surface of a water body, energy transfer in a wet cooling tower and the flow in a desert cooler, heat and mass transfer occur simultaneously. Possible applications of this type of flow can be found in many industries. For example, in the electric power industry, among the methods of generating electric power is one in which electrical energy is extracted directly from a moving conducting fluid. Muthucumaraswamy and Ganesan [18] studied the effect of the chemical reaction and injection on flow characteristics in an unsteady upward motion of an isothermal plate. Deka et al. [19] studied the effect of the first-order homogeneous chemical reaction on the process of an unsteady flow past an infinite vertical plate with a constant heat and mass transfer. Chamkha [20] studied the MHD flow of uniformly stretched vertical permeable surface in the presence of heat generation/absorption and a chemical reaction. Muthucumaraswamy and Ganesan [21] investigated the effects of a chemical reaction on the unsteady flow past an impulsively started semi-infinite vertical plate which subjected to uniform heat flux. Muthucumaraswamy and Ganesan [22] analyzed the effect of a chemical reaction on the unsteady flow past an impulsively started vertical plate which is subjected to uniform mass flux and in the presence of heat transfer. Muthucumaraswamy and Ganesan [23] studied the effects of suction on heat and mass transfer along a moving vertical surface in the presence of a chemical reaction. Raptis and Perdikis [24] analyzed the effect of a chemical reaction of an electrically conducting viscous fluid on the flow over a non-linearly (quadratic) semi-infinite stretching sheet in the presence of a constant magnetic field which is normal to the sheet. Seddeek et al. [25] analyzed the effects of chemical reaction, radiation and variable viscosity on hydromagnetic mixed convection heat and mass transfer for Hiemenz flow through porous media. Ibrahim et al. [26] analyzed the effects of the chemical reaction and radiation absorption on the unsteady MHD free convection flow past a semi-infinite vertical permeable moving plate with heat source and suction. In all these studies the fluids are assumed to be Newtonian.

Now, we propose to study the effect of the first-order chemical reaction and thermal radiation on the heat and mass transfer in MHD micropolar fluid flow over a vertical moving porous plate through a porous medium in the presence of heat generation. We also consider the free stream to consist of a mean velocity over which is superimposed an exponentially varying with time.

2. Formulation of the problem

We consider the two dimensional unsteady flow of a laminar, incompressible micropolar fluid past a semi-infinite vertical porous moving plate embedded in a uniform porous medium and subjected to a transverse magnetic field in the presence of a pressure gradient with chemical reaction and thermal radiation. The physical model and geometrical coordinates are shown in Fig. 1. The fluid is assumed to be a gray, absorping–emitting but non-scattering medium. The radiative heat flux in the x^*-direction is considered negligible in comparison that in the y^*-direction [27]. It is assumed that there is

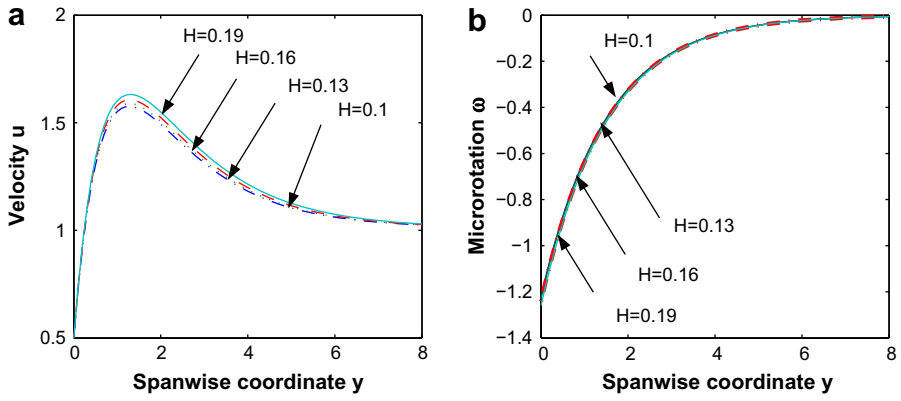

Fig. 3. Velocity and Microrotation profiles for various values of H with $n = 0.5$, $Sc = 0.2$, $M = 2$, $Gr = 2$, $Gc = 2$, $K = 2$, $Pr = 1$, $Up = 0.5$, $R = 0.1$, $\zeta = 1$ and $\beta = 0.5$.

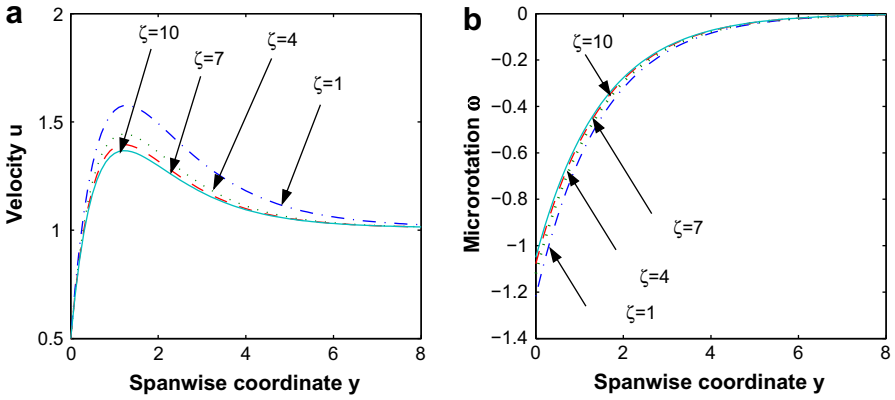

Fig. 4. Velocity and Microrotation profiles for various values of ζ with $n = 0.5$, $Sc = 0.2$, $M = 2$, $Gr = 2$, $Gc = 2$, $K = 2$, $Pr = 1$, $Up = 0.5$, $H = 0.1$, $R = 0.1$ and $\beta = 0.5$.

no applied voltage which implies the absence of an electric field. The transversely applied magnetic field and magnetic Reynolds number are very small and hence the induced magnetic field is negligible [28]. Viscous and Darcy resistance terms are taken into account the constant permeability porous medium. The MHD term is derived from an order-of-magnitude analysis of the full Navier–Stokes equations. It is assumed here that the hole size of the porous plate is significantly larger than a characteristic microscopic length scale of the porous medium. We regard the porous medium as an assemblage of small identical spherical particles fixed in space [29]. The fluid properties are assumed to be constants except that the influence of density variation with temperature and concentration has been considered in the body-force term. The concentration of diffusing species is very small in comparison to other chemical species, the concentration of species far from the wall C^*_∞, is infinitesimally small [30] and hence the Soret and Dufour effects are neglected. The chemical reactions are taking place in the flow and all thermo physical properties are assumed to be constant. Due to the semi-infinite plate surface assumption, furthermore, the flow variable are function of y^* and t^* only.

Under these assumptions the equations that describe the physical situation are given by

$$\frac{\partial v^*}{\partial y^*} = 0, \tag{1}$$

$$\frac{\partial u^*}{\partial t^*} + v^*\frac{\partial u^*}{\partial y^*} = -\frac{1}{\rho}\frac{\partial P^*}{\partial x^*} + (\nu + \nu_r)\frac{\partial^2 u^*}{\partial y^{*2}} + g\beta_f\left(T^* - T^*_\infty\right) + g\beta_c\left(C^* - C^*_\infty\right) - \frac{\nu u^*}{K^*} - \frac{\sigma}{\rho}B_0^2 u^* + 2\nu_r\frac{\partial \omega^*}{\partial y^*}, \tag{2}$$

$$\rho j^*\left(\frac{\partial \omega^*}{\partial t^*} + v^*\frac{\partial \omega^*}{\partial y^*}\right) = \gamma\frac{\partial^2 \omega^*}{\partial y^{*2}}, \tag{3}$$

$$\frac{\partial T^*}{\partial t^*} + v^*\frac{\partial T^*}{\partial y^*} = \frac{k}{\rho c_P}\frac{\partial^2 T^*}{\partial y^{*2}} + \frac{Q_0}{\rho c_P}\left(T^* - T^*_\infty\right) - \frac{1}{\rho c_P}\frac{\partial q^*_r}{\partial y^*}, \tag{4}$$

$$\frac{\partial C^*}{\partial t^*} + v^*\frac{\partial C^*}{\partial y^*} = D^*\frac{\partial^2 C^*}{\partial y^{*2}} - R^*\left(C^* - C^*_\infty\right). \tag{5}$$

The magnetic and viscous dissipations are neglected in this study. It is assumed that the porous plate moves with a constant velocity in the direction of fluid flow and the free stream velocity follows the exponentially increasing small perturbation law. In addition, it is assume that the temperature and concentration at the wall as well as the suction velocity are exponentially varying with time.

Under these assumptions, the appropriate boundary conditions for the velocity, temperature and concentration fields are

$$u^* = u^*_p, \quad T^* = T^*_w + \epsilon\left(T^*_w - T^*_\infty\right)e^{\delta^* t^*},$$
$$\omega^* = -n\frac{\partial u^*}{\partial y^*}, \quad C^* = C^*_w + \epsilon\left(C^*_w - C^*_\infty\right)e^{\delta^* t^*} \quad at\ y = 0, \tag{6}$$

$$u^* \to U^*_\infty = U_0\left(1 + \epsilon e^{\delta^* t^*}\right), \quad T^* \to T^*_\infty, \quad \omega^* \to 0,$$
$$C^* \to C^*_\infty \quad as\ y^* \to \infty \tag{7}$$

where, the variables and related quantities are defined above in the nomenclature.

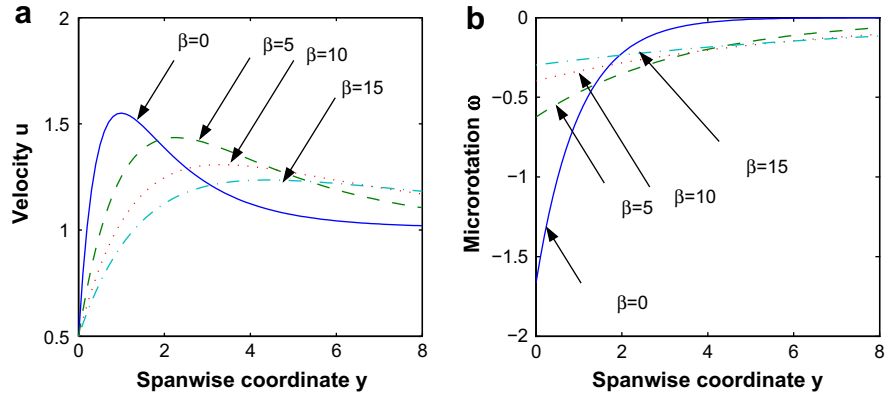

Fig. 5. Velocity and Microrotation profiles for various values of β with $n = 0.5$, $Sc = 0.2$, $M = 2$, $Gr = 2$, $Gc = 2$, $K = 2$, $Pr = 1$, $Up = 0.5$, $H = 0.1$, $R = 0.1$ and $\zeta = 0.5$.

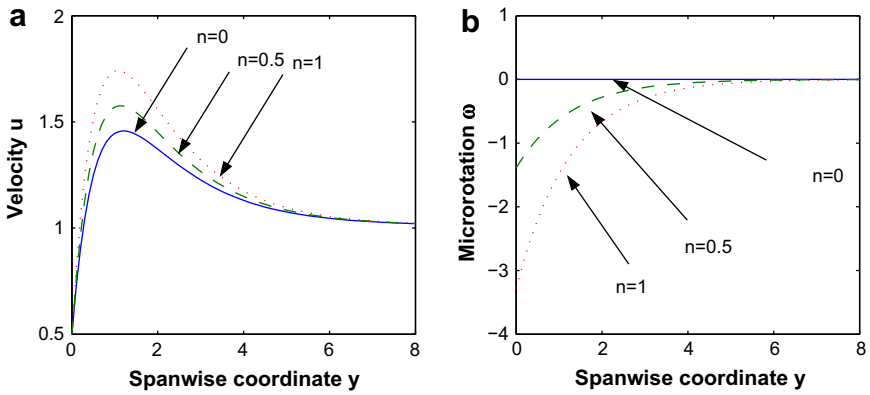

Fig. 6. Velocity and Microrotation profiles for various values of n with $\beta = 0.5$, $Sc = 0.2$, $M = 2$, $Gr = 2$, $Gc = 2$, $K = 2$, $Pr = 1$, $Up = 0.5$, $H = 0.1$, $R = 0.1$ and $\zeta = 1$.

The boundary condition for microrotation variable ω^* describes its relationship with the surface stress. In this equation, the parameter n is a number between 0 and 1 that relates the micro-gyration vector to the shear stress. The values $n = 0$ corresponds to the case where the particle density is sufficiently large so that microelements close to the wall are unable to rotate. The value $n = 0.5$ is indicative of weak concentrations, and when $n = 1$ flows are believed to represent turbulent boundary layers [31].

From the continuity equation (1), it is clear that the suction velocity normal to the plate is a function of time only and we shall take it in the form:

$$v^* = -V_o\left(1 + \epsilon A e^{\delta^* t^*}\right) \tag{8}$$

where, A is a real positive constant; ϵA small less than unity and V_o is a scale of suction velocity which has non-zero positive constant. Outside the boundary layer, equation (2) gives

$$-\frac{1}{\rho}\frac{\partial P^*}{\partial x^*} = \frac{\mathrm{d}U_\infty^*}{\mathrm{d}t^*} + \frac{\nu}{K^*}U_\infty^* + \frac{\sigma}{\rho}B_0^2 U_\infty^*. \tag{9}$$

The radiative heat flux term by using the Rosseland approximation is given by

$$q_r^* = -\frac{4\sigma^*}{3K_1^*}\frac{\partial T^{*4}}{\partial y^*} \tag{10}$$

We assume that the temperature difference within the flow are sufficiently small such that T^{*4} may be expressed as a linear function of the temperature. This is accomplished by expanding T^{*4} in a Taylor series about T_∞^* and neglecting higher-order terms, thus

$$T^{*4} \cong 4T_\infty^{*3}T^* - 3T_\infty^{*4}. \tag{11}$$

We now introduce the dimensionless variables as follows:

$$\left.\begin{aligned}
&u^* = U_0 u,\ \ v^* = V_0 v,\ \ u_P^* = U_0 U_P,\ \ y^* = \tfrac{\nu y}{V_0},\ \ U_\infty^* = U_0 U_\infty,\\
&\omega^* = \frac{\omega U_0 V_0}{\nu},\ \ J^* = \frac{J\nu^2}{V_0^2},\ \ t^* = \frac{\nu t}{V_0^2},\ \ T^* = T_\infty^* + \theta\left(T_w^* - T_\infty^*\right),\\
&C^* = C\left(C_w^* - C_\infty^*\right) + C_\infty^*,\ \ \delta^* = \frac{\delta V_0^2}{\nu},\ \ K^* = \frac{K\nu^2}{V_0^2},\ \ Sc = \frac{\nu}{D^*},\\
&H = \frac{\nu Q_0}{\rho c_P V_0^2},\ \ \zeta = \frac{R^*\nu}{V_0^2},\ \ M = \frac{\sigma B_0^2 \nu}{\rho V_0^2},\ \ Gr = \frac{\nu\beta_f g\left(T_w^* - T_\infty^*\right)}{V_0^2 U_0},\\
&Gc = \frac{\nu\beta_c g\left(C_w^* - C_\infty^*\right)}{V_0^2 U_0},\ \ Pr = \frac{\nu\rho c_P}{k} = \frac{\nu}{\alpha},\ \ R = \frac{4\sigma^* T_\infty^{*3}}{kK_1^*},\ \ \alpha = \frac{k}{\rho c_p}.
\end{aligned}\right\} \tag{12}$$

Furthermore, the spin-gradient viscosity γ which gives same relationship between the coefficients of viscosity and microinertia is defined as

$$\gamma = \left(\mu + \frac{\Gamma}{2}\right)j^* = \mu j^*\left(1 + \frac{\beta}{2}\right) \tag{13}$$

where,

$$\beta = \frac{\Gamma}{\mu}.$$

In view of equations (8)–(13), the governing equations (2)–(5) reduce to the following dimensionless form:

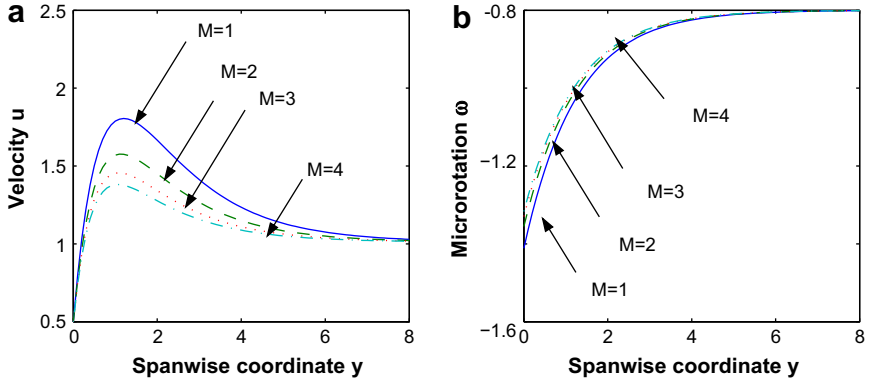

Fig. 7. Velocity and Microrotation profiles for various values of M with $\beta = 0.5$, $Sc = 0.2$, $n = 0.5$, $Gr = 2$, $Gc = 2$, $K = 2$, $Pr = 1$, $Up = 0.5$, $H = 0.1$, $R = 0.1$ and $\zeta = 1$.

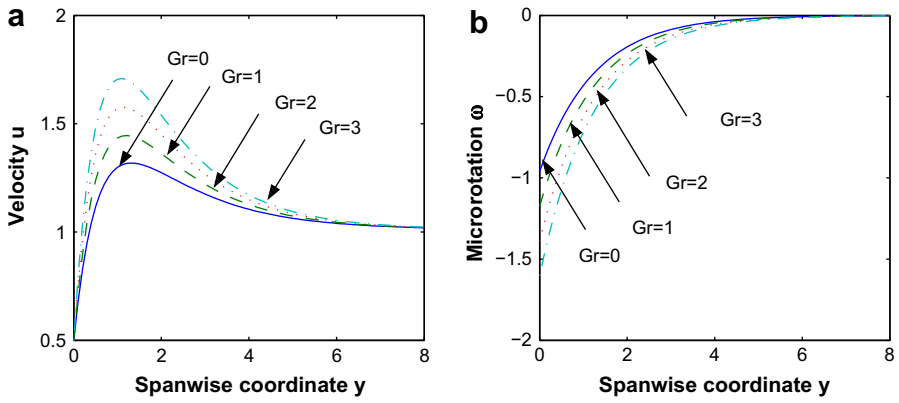

Fig. 8. Velocity and Microrotation profiles for various values of Gr with $\beta = 0.5$, $Sc = 0.2$, $M = 2$, $n = 0.5$, $Gc = 2$, $K = 2$, $Pr = 1$, $Up = 0.5$, $H = 0.1$, $R = 0.1$ and $\zeta = 1$.

$$\frac{\partial u}{\partial t} - \left(1 + \epsilon A e^{\delta t}\right)\frac{\partial u}{\partial y} = \frac{\mathrm{d}U_\infty}{\mathrm{d}t} + (1+\beta)\frac{\partial^2 u}{\partial y^2} + Gr\theta + GcC + N(U_\infty - u) + 2\beta\frac{\partial \omega}{\partial y}, \tag{14}$$

$$\frac{\partial \omega}{\partial t} - \left(1 + \epsilon A e^{\delta t}\right)\frac{\partial \omega}{\partial y} = \frac{1}{\eta}\frac{\partial^2 \omega}{\partial y^2}, \tag{15}$$

$$\frac{\partial \theta}{\partial t} - \left(1 + \epsilon A e^{\delta t}\right)\frac{\partial \theta}{\partial y} = \frac{1}{Pr}\left(1 + \frac{4R}{3}\right)\frac{\partial^2 \theta}{\partial y^2} + H\theta, \tag{16}$$

$$\frac{\partial C}{\partial t} - \left(1 + \epsilon A e^{\delta t}\right)\frac{\partial C}{\partial y} = \frac{1}{Sc}\frac{\partial^2 C}{\partial y^2} - \zeta C \tag{17}$$

where,

$$N = \left(M + \frac{1}{K}\right), \quad \eta = \frac{2}{2+\beta} = \frac{\mu j^*}{\gamma}. \tag{18}$$

The boundary conditions (6) and (7) are then given by the following dimensionless form:

$$u = U_P, \quad \theta = 1 + \epsilon e^{\delta t}, \quad \omega = -n\frac{\partial u}{\partial y}, \quad C = 1 + \epsilon e^{\delta t} \quad at\ y = 0, \tag{19}$$

$$u \to U_\infty \to \left(1 + \epsilon e^{\delta t}\right), \quad \theta \to 0, \quad \omega \to 0, \quad C \to 0, \quad as\ y \to \infty. \tag{20}$$

3. Analytical approximate solutions

In order to reduce the above system of partial differential equations in dimensionless form, we may represent the linear and angular velocities, temperature and concentration as

$$u = u_0(y) + \epsilon e^{\delta t} u_1(y) + O\left(\epsilon^2\right), \tag{21}$$

$$\omega = \omega_0(y) + \epsilon e^{\delta t} \omega_1(y) + O\left(\epsilon^2\right), \tag{22}$$

$$\theta = \theta_0(y) + \epsilon e^{\delta t} \theta_1(y) + O\left(\epsilon^2\right), \tag{23}$$

$$C = C_0(y) + \epsilon e^{\delta t} C_1(y) + O\left(\epsilon^2\right). \tag{24}$$

By substituting the above equations (21)–(24) into equations (14)–(17), equating the harmonic and non-harmonic terms and neglecting the higher-order terms of $O(\epsilon^2)$, we obtain the following pairs of equations for $(u_0, \omega_0, \theta_0, C_0)$ and $(u_1, \omega_1, \theta_1, C_1)$

$$(1+\beta)u_0'' + u_0' - Nu_0 = -N - Gr\theta_0 - GcC_0 - 2\beta\omega_0', \tag{25}$$

$$(1+\beta)u_1'' + u_1' - (N+\delta)u_1 = -(N+\delta) - Gr\theta_1 - GcC_1 - 2\beta\omega_1' - Au_0', \tag{26}$$

$$\omega_0'' + \eta\omega_0' = 0, \tag{27}$$

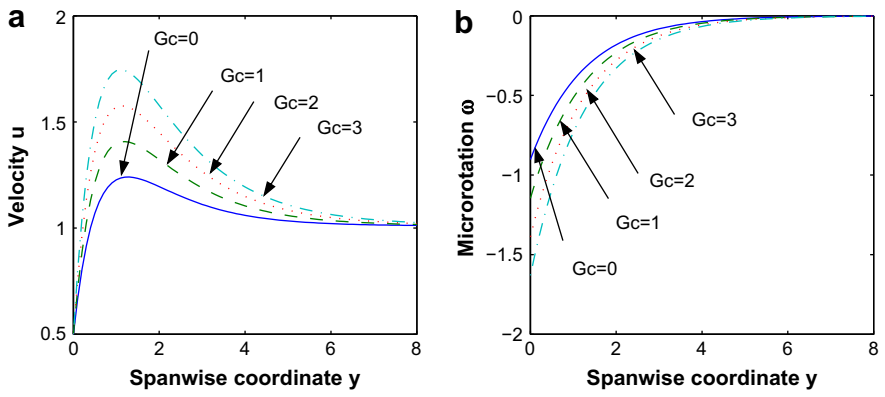

Fig. 9. Velocity and Microrotation profiles for various values of Gc with $\beta = 0.5$, $Sc = 0.2$, $M = 2$, $n = 0.5$, $Gr = 2$, $K = 2$, $Pr = 1$, $Up = 0.5$, $H = 0.1$, $R = 0.1$ and $\zeta = 1$.

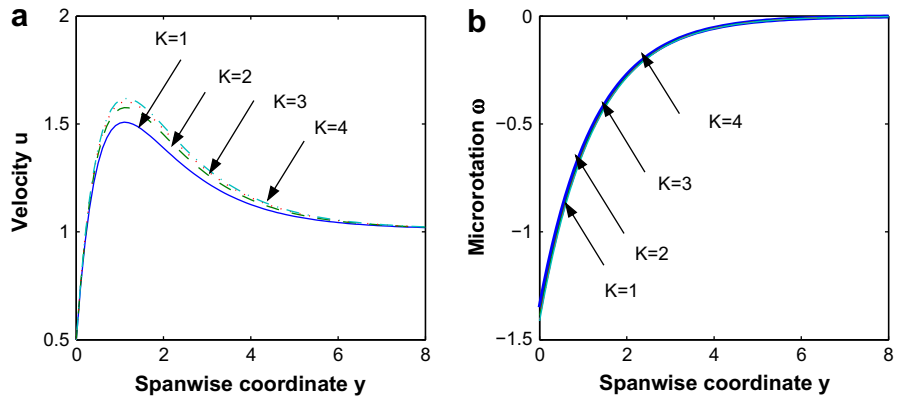

Fig. 10. Velocity and Microrotation profiles for various values of K with $\beta = 0.5$, $Sc = 0.2$, $M = 2$, $n = 0.5$, $Gc = 2$, $Gr = 2$, $Pr = 1$, $Up = 0.5$, $H = 0.1$, $R = 0.1$ and $\zeta = 1$.

$$\omega_1'' + \eta\omega_1' - \delta\eta\omega_1 = -A\eta\omega_0', \tag{28}$$

$$(3+4R)\theta_0'' + 3Pr(\theta_0' + H\theta_0) = 0, \tag{29}$$

$$(3+4R)\theta_1'' + 3Pr(\theta_1' - (\delta - H)\theta_1) = -3APr\theta_0', \tag{30}$$

$$C_0'' + ScC_0' - \zeta ScC_0 = 0, \tag{31}$$

$$C_1'' + ScC_1' - (\delta+\zeta)ScC_1 = -AScC_0' \tag{32}$$

where, the primes denote differentiation with respect to y.

The corresponding boundary conditions can be written as

$$u_0 = U_p, \quad u_1 = 0, \quad \omega_0 = -nu_0', \quad \omega_1 = -nu_1', \quad \theta_0 = 1, \quad \theta_1 = 1, \quad C_0 = 1, \quad C_1 = 1, \quad at\ y = 0 \tag{33}$$

and

$$u_0 \to 1, \quad u_1 \to 1, \quad \omega_0 \to 0, \quad \omega_1 \to 0, \quad \theta_0 \to 0, \quad \theta_1 \to 0, \quad C_0 \to 0, \quad C_1 \to 0 \quad as\ y \to \infty. \tag{34}$$

The solutions of equations (25)–(32) with satisfying boundary conditions (33) and (34) are given by

$$u_0(y) = 1 + a_1e^{-h_1y} + a_2e^{-R_1y} + a_3e^{-R_2y} + a_4e^{-\eta y}, \tag{35}$$

$$u_1(y) = 1 + b_1e^{-h_1y} + b_2e^{-h_2y} + b_3e^{-h_3y} + b_4e^{-h_4y} + b_5e^{-h_5y} + b_6e^{-R_1y} + b_7e^{-R_2y} + b_8e^{-\eta y}, \tag{36}$$

$$\omega_0(y) = -k_1e^{-\eta y}, \tag{37}$$

$$\omega_1(y) = -k_2e^{-h_5y} - \frac{\eta Ak_1}{\delta}e^{-\eta y}, \tag{38}$$

$$\theta_0(y) = e^{-R_1y}, \tag{39}$$

$$\theta_1(y) = (1-Z_1)e^{-h_3y} + Z_1e^{-R_1y}, \tag{40}$$

$$C_0(y) = e^{-R_2y}, \tag{41}$$

$$C_1(y) = e^{-h_4y} + Z_2\left(e^{-R_2y} - e^{-h_4y}\right) \tag{42}$$

where, the exponential indices and coefficients are given in Appendix A.

It is now important to calculate the physical quantities of primary interest, which are the local wall shear stress, the local surface heat and mass flux. Given the velocity field in the boundary layer, we can now calculate the skin-friction coefficient C_f at the wall, which given by

$$\tau_w^* = (\mu + \Gamma)\frac{\partial u^*}{\partial y^*}\Big|_{y^*=0} + \Gamma\omega^*\Big|_{y^*=0} \tag{43}$$

and in dimensionless form, we obtain

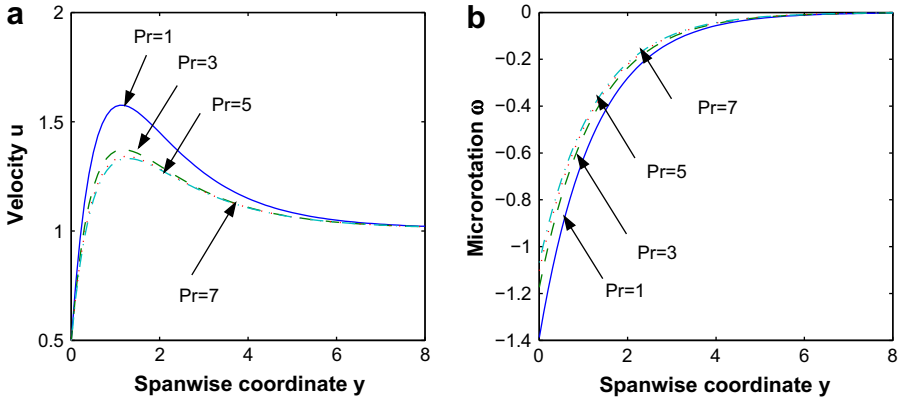

Fig. 11. Velocity and Microrotation profiles for various values of Pr with $\beta = 0.5$, $Sc = 0.2$, $M = 2$, $n = 0.5$, $Gc = 2$, $Gr = 2$, $K = 2$, $Up = 0.5$, $H = 0.1$, $R = 0.1$ and $\zeta = 1$.

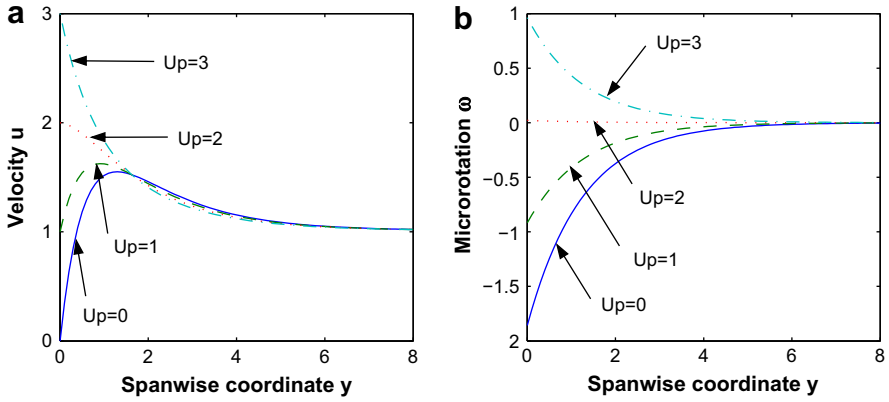

Fig. 12. Velocity and Microrotation profiles for various values of Up with $\beta = 0.5$, $Sc = 0.2$, $M = 2$, $n = 0.5$, $Gc = 2$, $Gr = 2$, $K = 2$, $Pr = 1$, $H = 0.1$, $R = 0.1$ and $\zeta = 1$.

$$C_f = \frac{2\tau_w^*}{\rho U_0 V_0} = 2[1 + (1-n)\beta]u'(0). \tag{44}$$

The couple stress coefficient (C_m) at the plate is written as

$$M_w = \gamma \left.\frac{\partial \omega^*}{\partial y^*}\right|_{y^*=0} \tag{45}$$

and in dimensionless form, we obtain

$$C_m = \frac{M_w}{\mu j U_0} = \left(1 + \frac{\beta}{2}\right)\omega'(0). \tag{46}$$

Knowing the temperature field, it is interesting to study the effect of the free convection and thermal radiation on the rate of heat transfer q_W^*, this is given by

$$q_w^* = -k\left(\frac{\partial T^*}{\partial y^*}\right)\Big|_{y^*=0} - \frac{4\sigma^*}{3K_1^*}\left(\frac{\partial T^{*4}}{\partial y^*}\right)\Big|_{y^*=0} \tag{47}$$

by using equation (11), q_W^* take the form

$$q_w^* = \left(-k + \frac{16\sigma^* T^{*3}}{3K_1^*}\right)\left.\frac{\partial T^*}{\partial y^*}\right|_{y^*=0} \tag{48}$$

which is written in dimensionless form as

$$q_w^* = \left(\frac{-k\left(T_w^* - T_\infty^*\right)V_0}{\nu}\right)\left(1 + \frac{4R}{3}\right)\left.\frac{\partial \theta}{\partial y}\right|_{y=0} \tag{49}$$

the dimensionless local surface heat flux (i.e., Nusselt number) is obtained as

$$Nu_x = \frac{x q_w^*}{k\left(T_w^* - T_\infty^*\right)} \tag{50}$$

where,

$$Nu_x Re_x^{-1} = -\left(1 + \frac{4R}{3}\right)\left.\frac{\partial \theta}{\partial y}\right|_{y=0},$$

$$Re_x = \frac{V_0 x}{\nu}.$$

The definition of the local mass flux and the local Sherwood number are respectively given by

$$j_w = -D^*\left(\frac{\partial C^*}{\partial y^*}\right)_{y^*=0}, \tag{51}$$

$$Sh_x = \frac{x j_w}{D^*\left(C_w^* - C_\infty^*\right)} \tag{52}$$

with the help of these equations, one can write

$$Sh_x Re_x^{-1} = -\left(\frac{\partial C}{\partial y}\right)_{y=0}. \tag{53}$$

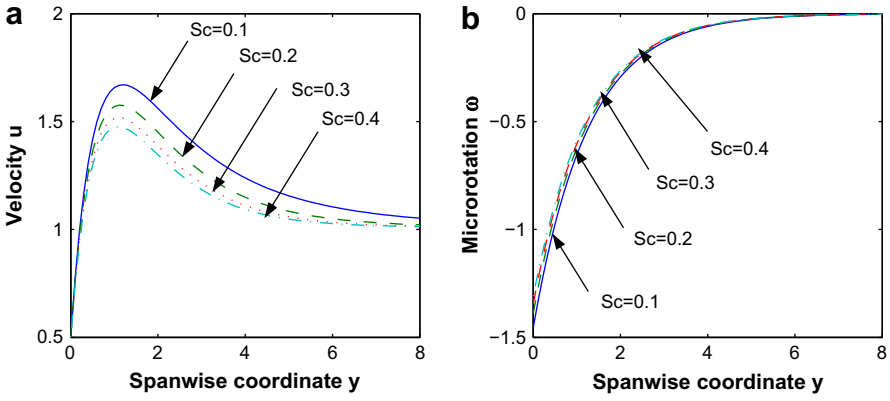

Fig. 13. Velocity and Microrotation profiles for various values of Sc with $\beta = 0.5$, $Pr = 1$, $M = 2$, $n = 0.5$, $Gc = 2$, $Gr = 2$, $K = 2$, $Up = 0.5$, $H = 0.1$, $R = 0.1$ and $\zeta = 1$.

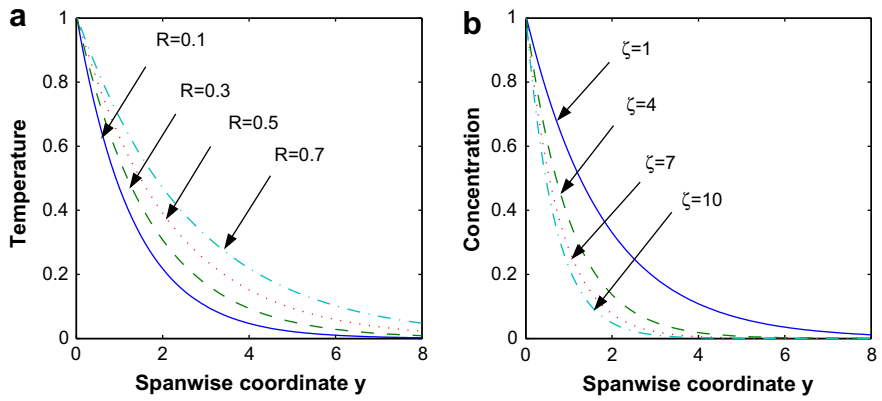

Fig. 14. a. Temperature profiles for various values of R with $\beta = 0.5$, $Sc = 0.2$, $M = 2$, $n = 0.5$, $Gc = 2$, $Gr = 2$, $K = 2$, $Up = 0.5$, $H = 0.1$, $Pr = 1$ and $\zeta = 1$. b. Concentration profiles for various values of ζ with $\beta = 0.5$, $Sc = 0.2$, $M = 2$, $n = 0.5$, $Gc = 2$, $Gr = 2$, $K = 2$, $Up = 0.5$, $H = 0.1$, $Pr = 1$ and $R = 0.1$.

It should be mentioned that in the absence of the chemical reaction, heat source and thermal radiation effects, the relevant results obtained are deduced as the results obtained by Kim [32].

4. Numerical results and discussions

The formulation of the effect of chemical reaction and thermal radiation on MHD convective flow and mass transfer of an incompressible, micropolar fluid along a semi-infinite vertical porous moving plate in a porous medium in the presence of heat generation has been performed in the preceding sections. This enables us to carry out the numerical calculations for the distribution of the translational velocity, microrotation, temperature and concentration across the boundary layer for various parameters. In the present study we have chosen $t = 1$, $\delta = 0.01$, $\epsilon = 0.01$ and $A = 0.1$, while R, H, ζ, β, n, M, Gr, Gc, Pr, U_P and Sc are varied over a range, which are listed in the figure legends. In the present study the boundary conditions for $y \to \infty$ is replaced by identical ones at y max which is a sufficiently large value of y where the velocity profiles u approaches the relevant free stream velocity. We choose y max $= 8$ and a step size $\Delta y = 0.001$.

For different values of radiation parameter R, the translational velocity and microrotation profiles are plotted in Fig. 2. It is obvious that velocity distribution across the boundary layer increases with the increasing values of R-parameter. The results also show that the magnitude of microrotation on the porous plate increases slightly as R-parameter increases. The effects of heat generation H on the translational velocity and microrotation profiles across the boundary layer are presented in Fig. 3. It is shown that the translational velocity across the boundary layer increases with an increasing of H. Also, it is appear that there is a slight change on microrotation as H increases. Fig. 4 shows the translational velocity and the microrotation profiles across the boundary layer for various values of the chemical reaction parameter ζ. The results display that with an increasing of ζ, the translational velocity decreases but the magnitude of microrotation increases as ζ decreases and then approach to the free stream boundary layer conditions. The effects of viscosity ratio β on the translational velocity and the microrotation profiles across the boundary layer are presented in Fig. 5, it is clear that the velocity distribution is greater for a Newtonian fluid ($\beta = 0$) with the fixed flow and material parameters, as compared with micropolar fluids until its peak value reaches.

The translational velocity distribution shows a decelerating nature near the porous plate as β – parameter increases, and then decays to the relevant free stream velocity. Furthermore, the magnitude of microrotation at the wall decreased as β – parameter increases. Fig. 6 shows the effect of n – parameter, which is related to microrotation vector and shear stress, on the translational velocity and the microrotation profiles. It is observed that the magnitude of velocity increases with an increasing of n – parameter but the magnitude of microrotation increases with an increasing of n – parameter.

For various values of magnetic field parameter M, the translational velocity and microrotation profiles are plotted in Fig. 7. It is obvious that with increasing values of M – parameter, the velocity distribution across the boundary layer decreases. Because of the application of transverse magnetic field will result a restrictive type force (Lorenz's force) similar to drag force which tends to resist the fluid flow and thus reducing its velocity. The results also show that

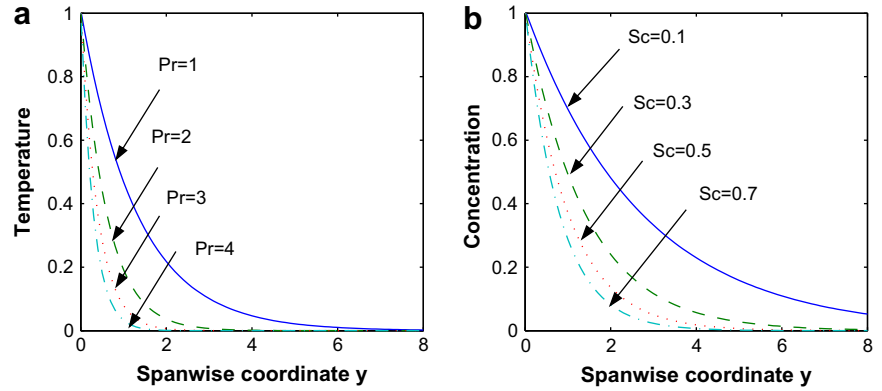

Fig. 15. a. Temperature profiles for various values of Pr with $\beta = 0.5$, $Sc = 0.2$, $M = 2$, $n = 0.5$, $Gc = 2$, $Gr = 2$, $K = 2$, $Up = 0.5$, $H = 0.1$, $R = 0.1$, and $\zeta = 1$. b. Concentration profiles for various values of Sc with $\zeta = 1$, $M = 2$, $n = 0.5$, $\beta = 0.5$, $Gc = 2$, $Gr = 2$, $K = 2$, $Up = 0.5$, $H = 0.1$, $Pr = 1$ and $R = 0.1$.

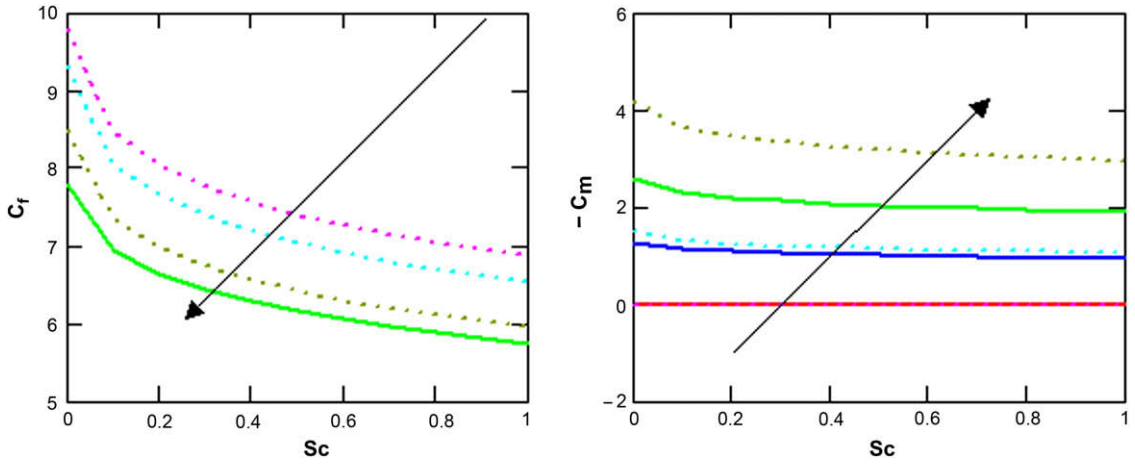

Fig. 16. Effect of n on C_f and $-C_m$ respect Sc, where, $R = H = 0.1$, $\zeta = Pr = 1$, $n = 0$, 0.5, 1 and $\beta = 0$—, $\beta = 1$….

the magnitude of microrotation on the porous plate is increased as M – parameter decreases.

The translational velocity and the microrotation profiles against spanwise coordinate y for different values of thermal Grashof number Gr and solutal Grashof number Gc are displayed in Figs. 8 and 9, respectively. It is observed that an increasing in Gr or Gc leads to increasing in the values of velocity and increasing in the magnitude of microrotation. For various values of the permeability K, the profiles of translational velocity and the microrotation across the boundary layer are shown in Fig. 10. It is clearly as K increases, the translational velocity profiles across the boundary layer increases. The results also show that there is a slight change on microrotation with the various values of K. Fig. 11 shows the translational velocity and the microrotation profiles across the boundary layer for different values of Prandtl number Pr. It is appear that with an increasing of Pr, the translational velocity and the magnitude of microrotation are decreased at the wall and then approach to the free stream boundary layer conditions. It is also noted that the magnitude of microrotation profiles decreases as Pr increases. Fig. 12 displays the variation of velocity and microrotation distribution

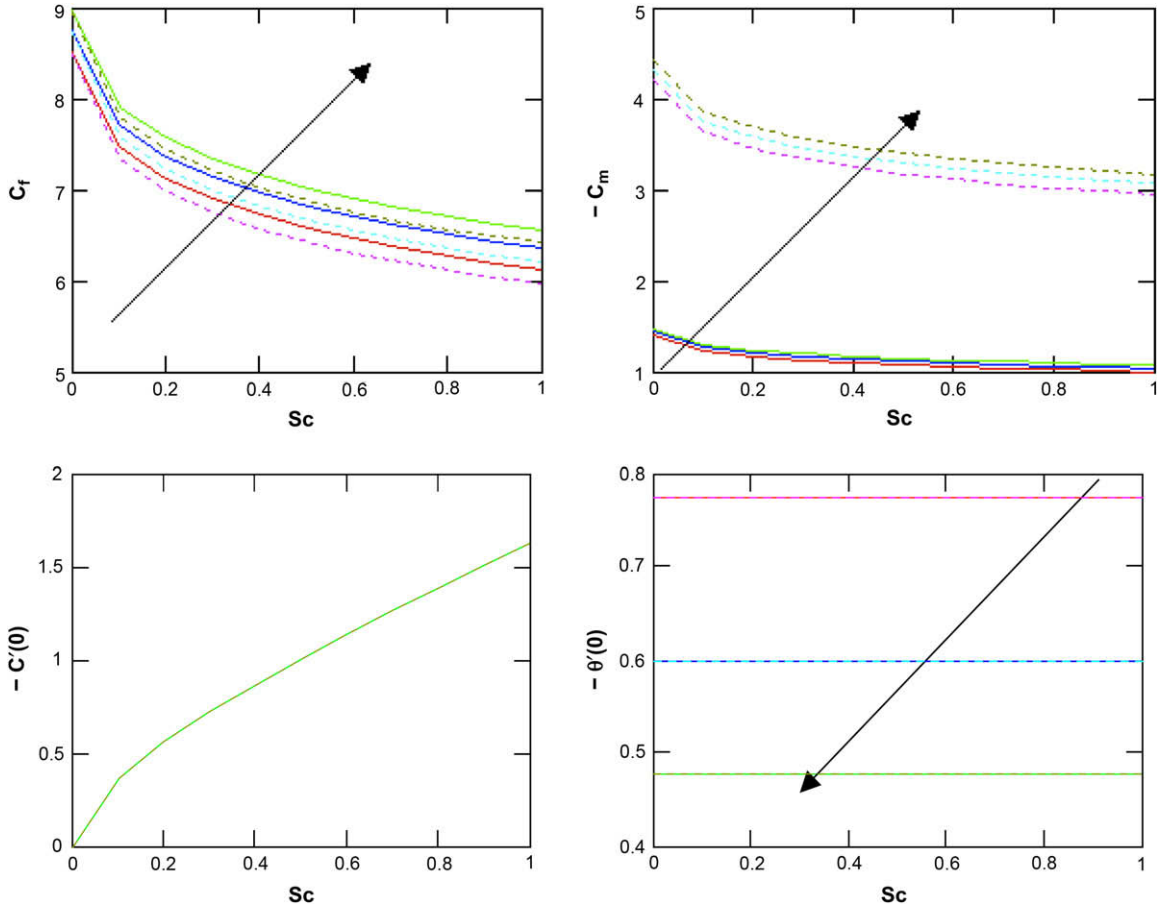

Fig. 17. Effect of R on C_f, C_m, $-C'(0)$ and $-\theta'(0)$ respect Sc, where, $H = 0.1$, $\zeta = Pr = 1$, $R = 0.1$, 0.3, 0.5 and $\beta = n = 0.5$—, $\beta = n = 1$….

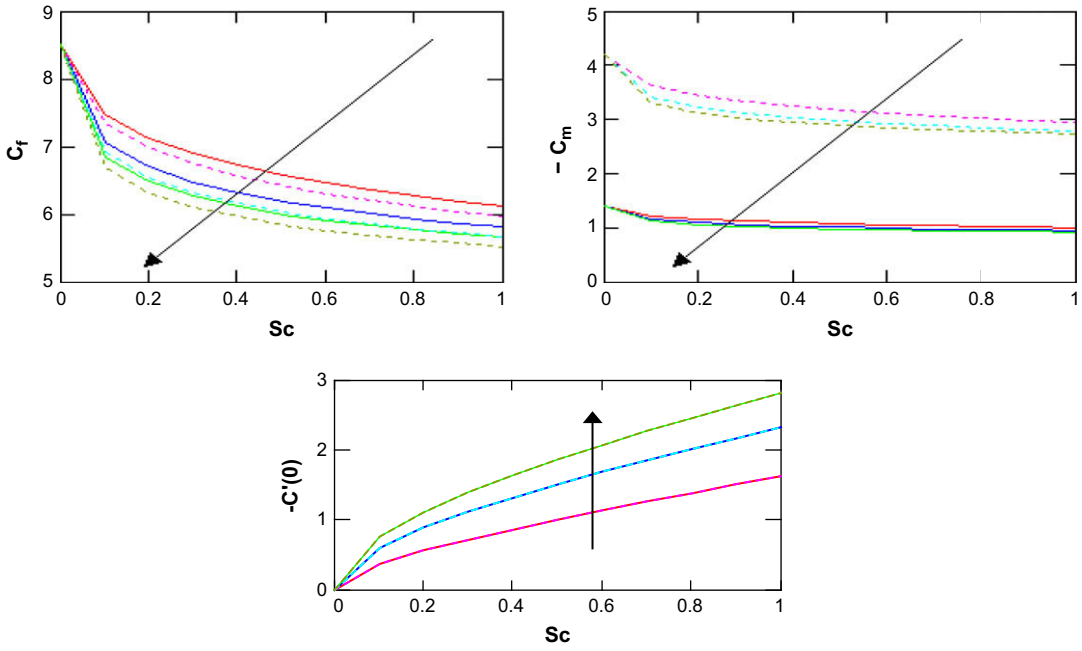

Fig. 18. Effect of R on C_f, $-C_m$ and $-C'(0)$ respect Sc, where, $Pr = 1$, $H = R = 0.1$, $\zeta = 1, 3, 5$ and $\beta = n = 0.5$—, $\beta = n = 1$….

across the boundary layer for various values of the plate velocity U_P in the direction of fluid flow. It is obvious that the values of translational velocity and microrotation on the porous plate are increased as the plate increases, and then decayed of the free stream velocity. For various values of the Schmidt number Sc, the translational velocity and microrotation profiles are plotted in Fig. 13. It is obvious that the increased values of Sc tend to decreasing of the velocity distribution across the boundary layer. Furthermore, the results show that the magnitude of microrotation on the porous plate decreases slightly as Sc increases.

Typical variations of the temperature profiles along the spanwise coordinate y are shown in Fig. 14a for varies values of thermal radiation parameter R. The results show that as an increasing of thermal radiation parameter the temperature profiles increases. For different values of the chemical reaction parameter ζ, the concentration profiles plotted in Fig. 14b. It is obvious that the influence of increasing values of ζ, the concentration distribution across the boundary layer decreases. Hence, the concentration boundary layer thin as reaction parameter increases. Fig. 15a shows the temperature profiles respect to spanwise coordinate y for various values of Prandtl number Pr. The results show that as an increasing of Prandtl number Pr, the thermal boundary layer decreases. The reason is that smaller values of Pr are equivalent to increasing of the thermal conductivities, and therefore heat is able to diffuse away from the heated surface more rapidly than for higher values of Pr. Fig. 15b shows the concentration profiles across Schmidt number Sc. It is shown that with an increasing of Sc, the concentration distribution decreases, because the smaller values of Sc are equivalent the increasing the chemical molecular diffusivity. From Fig. 16, it is appear that C_f decreases with an increasing of Sc, doesn't affect with the various values of n if $\beta = 0$ but decreases with an increasing of n if $\beta = 1$. Also, it is seen that $-C_m = 0$ if ($n = 0$ and $\beta = \{0, 1\}$) with varies values of Sc but decreases with another values of n and β, with an increasing of n and β, it is shown that $-C_m$ increases.

By computational work, it is concluded that concentration $C'(0)$ increases from zero with varies values of Sc and not influence with

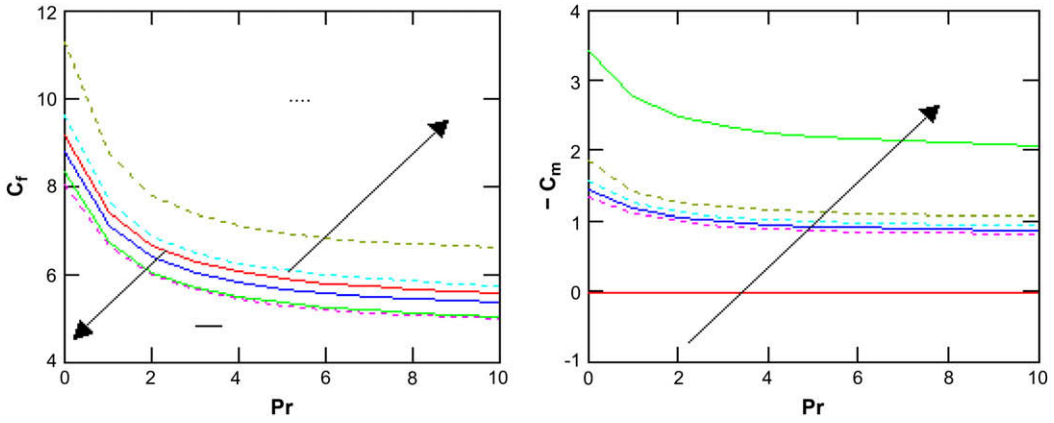

Fig. 19. Effect of n and β on C_f and $-C_m$ respect Pr, where, $Sc = 0.2$, $H = R = 0.1$, $\zeta = 1$ and $n = 0, 0.5, 1$—, $\beta = 0, 1, 2$….

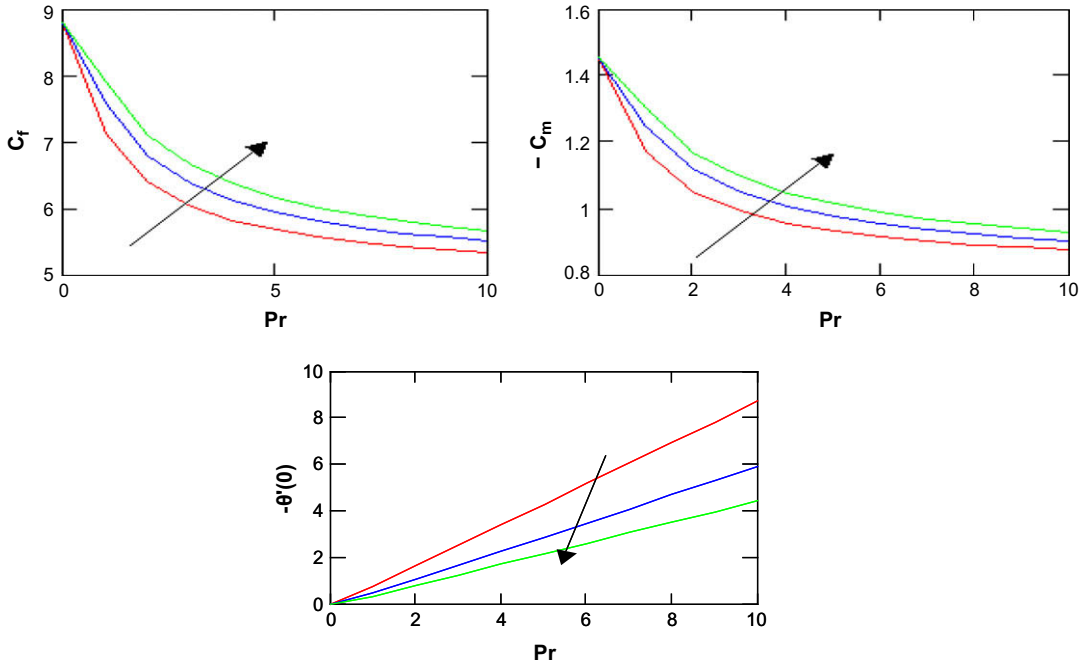

Fig. 20. Effect of R on C_f, $-C_m$ and $-\theta'(0)$ respect Pr, where, $Sc = 0.2$, $\zeta = 1$, $H = 0.1$, $R = 0.1, 0.5, 0.9$ and $\beta = n = 0.5$.

varies values of n and β, also, $-\theta'(0)$ equal 0.879 with various values of Sc, n and β. From Fig. 17, it is seen that C_f and $-C_m$ decrease with an increasing of Sc, increase with an increasing of R, also, it is appear that $-C'(0)$ increases from zero with varies values of Sc and doesn't affect by varies values values of R. Finally, it is shown that $-\theta'(0)$ decreases with an increasing of R and doesn't affect with an increasing of Sc. Also, it is shown that the effects of H in C_f, $-C_m$, $-C'(0)$ and $-\theta'(0)$ take the same path of the influence of R.

From Fig. 18, it is seen that C_f and $-C_m$ decrease with an increasing of Sc, decrease with an increasing of ζ, also, it is appear that $-C'(0)$ increases from zero with varies values of Sc and increases with an increasing of ζ, also, it is shown that

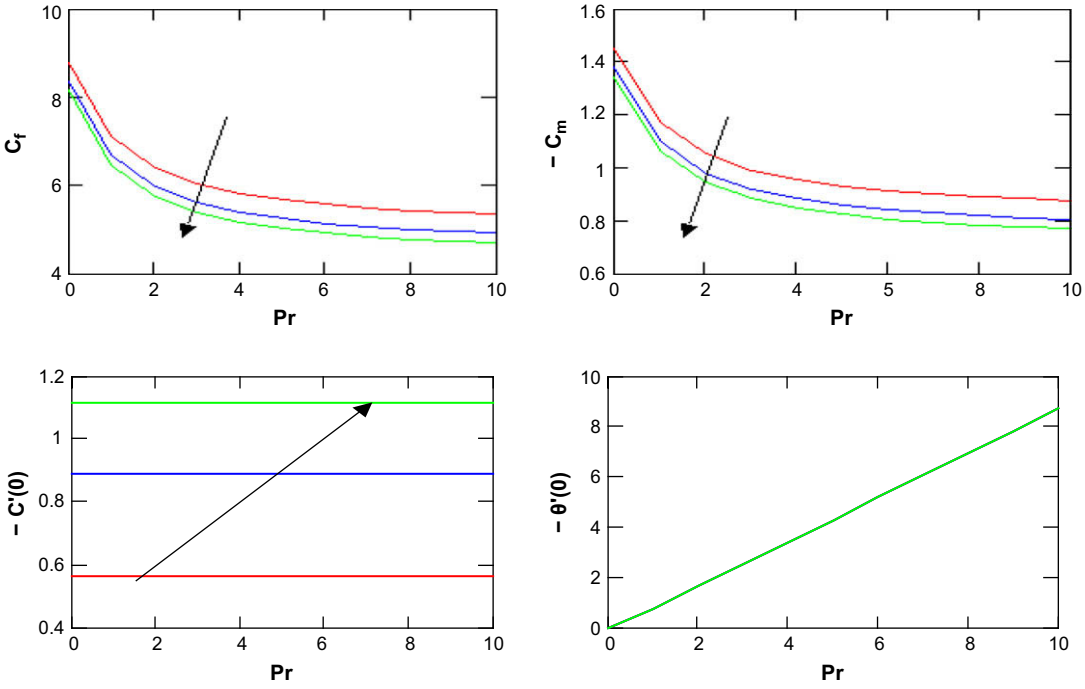

Fig. 21. Effect of ζ on C_f, $-C_m$, $-C'(0)$ and $-\theta'(0)$ respect Pr, where, $Sc = 0.2$, $R = H = 0.1$, $\zeta = 1, 3, 5$ and $\beta = n = 0.5$.

$-\theta'(0)=0.879$ with varies values of Sc and ζ. From Fig. 19, it is seen that C_f decreases with an increasing of Pr and n but increases with an increasing of β, also, it is appear that $-C_m=0$ if $n=0$ with varies values of Pr and decreases with varies values of Pr, n and β.

Finally, it is shown that $C'(0)=0.564$ with varies values of Pr, n and β but $\theta'(0)$ increases with increasing of Pr and does not affect with increasing of n and β. From Fig. 20, it is shown that C_f and $-C_m$ are decreased with an increasing of Pr and increased with an increasing of R, vice versa respect to $-\theta'(0)$. Also, it is pointed out $-C'(0)=0.564$ with the varies values of Pr and R. From Fig. 21, it is appear that C_f and $-C_m$ are decreased with an increasing of Pr and ζ but $-C'(0)$ doesn't affect with the varies values of Pr and increases with an increasing of ζ. Also, it is shown that $-\theta'(0)$ increases with an increasing of Pr and doesn't influence by the varies values of ζ.

5. Conclusion

In this paper, we have theoretically studied the effects of chemical reaction and thermal radiation on unsteady MHD convective flow and mass transfer of an incompressible, micropolar fluid along a semi-infinite vertical porous moving plate in a porous medium in the presence of heat generation. The method of solution can be applied for small perturbation. Numerical results are presented to illustrate the details of the flow, heat and mass transfer characteristics and their dependence on material parameters. We observe that, the translational velocity across the boundary layer and the magnitude of microrotation at the wall are decreased with an increasing values of ζ, M, Sc, β and Pr, while they show opposite trends with an increasing values of R, H, n, Gr, Gc and K. We may conclude that, the temperature increases as R increases and decreases as Pr increases. The concentration decreases as ζ and Sc decreases. It is hoped that the results obtained will not only provide useful information for applications, but also serve as a complement to the previous studies.

Appendix A

The exponential indices in Eqs. (35)–(42) are defined by

$$
\begin{aligned}
h_1 &= \frac{1}{2(1+\beta)}\left[1+\sqrt{1+4N(1+\beta)}\right],\\
h_2 &= \frac{1}{2(1+\beta)}\left[1+\sqrt{1+4(\delta+N)(1+\beta)}\right],\\
h_3 &= \frac{3Pr}{2(3+4R)}\left[1+\sqrt{1+\frac{4(\delta-H)(3+4R)}{3Pr}}\right],\\
h_4 &= \frac{Sc}{2}\left[1+\sqrt{1+\frac{4(\delta+\zeta)}{Sc}}\right],\\
h_5 &= \frac{\eta}{2}\left[1+\sqrt{1+\frac{4\delta}{\eta}}\right],\\
R_1 &= \frac{3Pr}{2(3+4R)}\left[1+\sqrt{1-\frac{4H(3+4R)}{3Pr}}\right],\\
R_2 &= \frac{Sc}{2}\left[1+\sqrt{1-\frac{4\zeta}{Sc}}\right]
\end{aligned}
$$

and the coefficients are given by

$$
\begin{aligned}
a_1 &= U_P-1-a_2-a_3-a_4,\\
a_2 &= \frac{-Gr}{(1+\beta)R_1^2-R_1-N},\\
a_3 &= \frac{-Gc}{(1+\beta)R_2^2-R_2-N},\\
a_4 &= \frac{2\beta\eta k_1}{(1+\beta)\eta^2-\eta-N} = \Theta k_1,\\
Z_1 &= \frac{3APrR_1}{(3+4R)R_1^2-3PrR_1-3(\delta-H)Pr},\\
Z_2 &= \frac{AScR_2}{R_2^2-ScR_2-(\delta+D)Sc},
\end{aligned}
$$

$$
\begin{aligned}
b_1 &= \frac{Aa_1h_1}{(1+\beta)h_1^2-h_1-(\delta+N)},\\
b_2 &= -(1+b_1+b_3+b_4+b_5+b_6+b_7+b_8),\\
b_3 &= \frac{(Z_1-1)Gr}{(1+\beta)h_3^2-h_3-(\delta+N)},\\
b_4 &= \frac{(Z_2-1)Gc}{(1+\beta)h_4^2-h_4-(\delta+N)},\\
b_5 &= \frac{2\beta h_5}{(1+\beta)h_5^2-h_5-(\delta+N)}k_2 = \Psi k_2,\\
b_6 &= \frac{Aa_2R_1-GrZ_1}{(1+\beta)R_1^2-R_1-(\delta+N)},\\
b_7 &= \frac{Aa_3R_2-GcZ_2}{(1+\beta)R_2^2-R_2-(\delta+N)},\\
b_8 &= \eta A\left(a_4-\frac{2\beta\eta k_1}{\delta}\right)\frac{1}{(1+\beta)\eta^2-\eta-(\delta+N)},\\
k_1 &= \frac{n}{1+n(h_1-\eta)\Theta}\left[(u_p-1)h_1+(R_1-h_1)a_2+(R_2-h_1)a_3\right],\\
k_2 &= \frac{1}{1-h_5\Psi}\left[\frac{A\eta k_1}{\delta}+n(b_1h_1+b_2h_2+b_3h_3+b_4h_4\right.\\
&\quad \left.+b_6R_1+b_7R_2+b_8\eta)\right].
\end{aligned}
$$

References

[1] A.C. Eringen, Theory of micropolar fluids, J. Math. Mech. 16 (1966) 1–16.
[2] A.C. Eringen, Theory of thermomicropolar fluids, J. Math. Anal. Appl. 38 (1972) 480–496.
[3] G. Lukaszewicz, Micropolar Fluids: Theory and Applications, Birkhäuser, Boston, MA, 1999.
[4] A. Raptis, Boundary layer flow of micropolar fluids in porous medium, J. Porous Media 3 (2000) 95–97.
[5] K.A. Helmy, Unsteady free convection flow past a vertical porous plate, ZAMM 78 (4) (1998) 255–270.
[6] Y.J. Kim, Unsteady convection flow of micropolar fluids past a vertical porous medium, Acta Mech. 148 (1–4) (2001) 106–116.
[7] I. Aganovic, Z. Tutek, Homogenization of micropolar fluid through a porous medium, in: A. Bourgeat, et al. (Eds.), Mathematical Modeling of Flow Through Porous Media, World Scientific, 1995, pp. 3–13.
[8] R.C. Sharma, U. Gupta, Thermal convection in micropolar fluids in porous medium, Int. J. Eng. Sci. 33 (1995) 1887–1892.
[9] I.A. Hassanien, A.H. Essawy, N.M. Moursy, Natural convection flow of micropolar fluid from a permeable uniform heat flux surface in a porous medium, Appl. Math. Comput. 152 (2004) 323–335.
[10] F.S. Ibrahim, I.A. Hassanien, A.A. Baker, Nonclassical thermal effects in Stokes's second problem for micropolar fluids, ASME J. Appl. Mech. 23 (2005) 468–474.
[11] F.S. Ibrahim, I.A. Hassanien, A.A. Baker, Unsteady magneto-hydrodynamic micropolar fluid flow and heat transfer over a vertical porous medium in the presence of thermal and mass diffusion with constant heat source, Can. J. Phys. 82 (2004) 775–790.
[12] Y.J. Kim, Unsteady MHD convection flow of polar fluids past a vertical moving porous plate in a porous medium, Int. J. Heat Mass Transfer 44 (2001) 2791–2799.
[13] A. Raptis, Flow of a micropolar fluid past a continuously moving plate by the presence of radiation, Int. J. Heat Mass Transfer 41 (1998) 2865–2866.
[14] E.M. Abo-Eldahab, A.F. Ghonaim, Radiation effect on heat transfer of a micropolar fluid through a porous medium, Appl. Math. Comput 169 (2005) 500–510.
[15] Y.J. Kim, A.G. Fedorov, Transient mixed radiative convection flow of micropolar fluid past a moving semi-infinite vertical porous plate, Int. J. Heat Mass Transfer 46 (2003) 1751–1758.
[16] E.M. Abo-Eldahab, M.A. El-Aziz, Flow and heat transfer in a micropolar fluid past a stretching surface embedded in a non-Darcing porous medium with uniform free stream, Appl. Math. Comput 162 (2005) 881–899.
[17] R.S.R. Gorla, A.A. Mohammedien, M.A. Mansour, I.A. Hassanien, Unsteady natural convection from a heated vertical plate in micropolar fluid, Numer. Heat Transfer, Part A 28 (1995) 253–262.
[18] R. Muthucumaraswamy, P. Ganesan, Effect of the chemical reaction and injection on flow characteristics in an unsteady upward motion of an isothermal plate, J. Appl. Mech. Tech. Phys. 42 (2001) 665–671.
[19] R. Deka, U.N. Das, V.M. Soundalgekar, Effects of mass transfer on flow past an impulsively started infinite vertical plate with constant heat flux and chemical reaction, Forschung Ingenieurwesen 60 (1994) 284–287.
[20] A.J. Chamkha, MHD flow of uniformly stretched vertical permeable surface in the presence of heat generation/absorption and a chemical reaction, Int. Comm. Heat Mass Transfer 30 (2003) 413–422.
[21] R. Muthucumaraswamy, P. Ganesan, On impulsive motion on a vertical plate with heat flux and diffusion on chemically reactive species, Forschung Ingenieurwesen 66 (2000) 17–23.
[22] R. Muthucumaraswamy, P. Ganesan, First-order chemical reaction on flow past on impulsively started vertical plate with uniform heat and mass flux, Acta Mech. 147 (2001) 1–13.

[23] R. Muthucumaraswamy, P. Ganesan, Effects of suction on heat and mass transfer along a moving vertical surface in the presence of chemical reaction, Forschung Ingenieurwesen 67 (2002) 129–132.
[24] A. Raptis, C. Perdikis, Viscous flow over a non-linearly stretching sheet in the presence of a chemical reaction and magnetic field, Int. J. Non Lin. Mech. 41 (2006) 527–529.
[25] M.A. Seddeek, A.A. Darwish, M.S. Abdelmeguid, Effects of chemical reaction and variable viscosity on hydromagnetic mixed convection heat and mass transfer for Hiemenz flow through porous media with radiation, Comm. Nonlinear Sci. Numer. Simulat. 12 (2007) 195–213.
[26] F.S. Ibrahim, A.M. Elaiw, A.A. Bakr, Effect of the chemical reaction and radiation absorption on the unsteady MHD free convection flow past a semi-infinite vertical permeable moving plate with heat source and suction, Comm. Nonlinear Sci. Numer. Simulat. 13 (2008) 1056–1066.
[27] E.M. Sparrow, R.D. Cess, Radiation Heat Transfer, Augmented Edition, Hemisphere Publishing Corp., Washington DC, 1978, (Chapters 7 and 10).
[28] T.G. Cowling, Magnetohydrodynamics, Interscience Pubishers, New York, 1957.
[29] K. Yamamoto, N. Iwmura, Flow with convective acceleration through a porous medium, J. Eng. Math. 10 (1976) 41–54.
[30] R. Byron Bird, Warren E. Stewart, Edwin N. Lightfoot, Transfer phenomena, John Wiley & Sons, New York, 1992, p. 605.
[31] D.A.S. Rees, A.P. Basson, The Blassius boundary layer flow of a micropolar fluid, Int. J. Eng. Sci. 34 (1) (1996) 113–124.
[32] Y.J. Kim, Heat and mass transfer in MHD micropolar flow over a vertical moving porous plate in a porous medium, Transport Porous Media 56 (2004) 17–37.